PARALLEL FINITE ELEMENT PARTICLE-IN-CELL CODE FOR SIMULATIONS OF SPACE-CHARGE DOMINATED BEAM-CAVITY INTERACTIONS*

A. Candel[†], A. Kabel, L. Lee, Z. Li, C. Limborg, C. Ng,
E. Prudencio, G. Schussman, R. Uplenchwar and K. Ko,
SLAC, Menlo Park, CA 94025, U. S. A.

Abstract

Over the past years, SLAC's Advanced Computations Department (ACD) has developed the parallel finite element (FE) particle-in-cell code Pic3P (Pic2P) for simulations of beam-cavity interactions dominated by space-charge effects. As opposed to standard space-charge dominated beam transport codes, which are based on the electrostatic approximation, Pic3P (Pic2P) includes space-charge, retardation and boundary effects as it self-consistently solves the complete set of Maxwell-Lorentz equations using higher-order FE methods on conformal meshes. Use of efficient, large-scale parallel processing allows for the modeling of photoinjectors with unprecedented accuracy, aiding the design and operation of the next-generation of accelerator facilities. Applications to the Linac Coherent Light Source (LCLS) RF gun are presented.

INTRODUCTION

The Office of Science in the U. S. DOE is promoting the use of High Performance Computing (HPC) in projects relevant to its mission via the 'Scientific Discovery through Advanced Computing' (SciDAC) program which began in 2001 [1]. Since 1996, SLAC has been developing a parallel accelerator modeling capability, first under the DOE Grand Challenge and now under SciDAC, for use on HPC platforms to enable the large-scale electromagnetic and beam dynamics simulations needed for improving existing facilities and optimizing the design of future machines.

METHODS

In the following, a brief introduction to the employed methods for simulating the full set of Maxwell's equations in time domain in the presence of charged particles is given.

Maxwell Finite Element Time-Domain

Ampere's and Faraday's laws can be combined to yield the (loss-less) inhomogeneous vector wave equation for the electric field:

$$\varepsilon \frac{\partial^2}{\partial t^2}\mathbf{E} + \nabla \times \mu^{-1}\nabla \times \mathbf{E} = -\frac{\partial}{\partial t}\mathbf{J}.$$

05 Beam Dynamics and Electromagnetic Fields

It can be integrated in time to obtain

$$\varepsilon \frac{\partial^2}{\partial t^2}\int_{-\infty}^{\mathbf{t}} \mathbf{E}\, d\tau + \nabla \times \mu^{-1}\nabla \times \int_{-\infty}^{\mathbf{t}} \mathbf{E}\, d\tau = -\mathbf{J}, \quad (1)$$

where $\mathbf{E}$ is the electric field intensity, $\mathbf{J}$ is the electric current source density, and ε and μ are the electric permittivity and magnetic permeability.

In our approach, $\int_{-\infty}^{t} \mathbf{E}\, d\tau$ in Eq. (1) is expanded into a set of localized hierarchical FE Whitney basis functions $\mathbf{N_i(x)}$

$$\int_{-\infty}^{t} \mathbf{E}(\mathbf{x}, \tau)\, d\tau = \sum_i e_i(t) \cdot \mathbf{N_i(x)} \quad (2)$$

up to order p. After accounting for boundary conditions and sharing of basis functions between neighboring elements, a global number of expansion coefficients is obtained, representing the (field) degrees of freedom (DOFs) of the system.

Substituting Eq. (2) into Eq. (1), multiplying by a test function and integrating over the computational domain Ω results in a matrix equation, second-order in time. The unconditionally stable implicit Newmark-Beta scheme [2] is employed for numerical time integration. It has been extended to support variable time steps. The resulting sparse positive definite system matrix is distributed over the compute nodes and can either be factorized with a direct solver or, if memory requirements or parallel scalability become an issue, with iterative methods and various preconditioners.

The electric field $\mathbf{E}$ and the magnetic flux density $\mathbf{B}$ are then easily obtained from the solution vector $\mathbf{e}$:

$$\mathbf{E(x)} = \sum_{\mathbf{i}} (\partial_{\mathbf{t}}\mathbf{e})_{\mathbf{i}} \cdot \mathbf{N_i(x)} \quad (3)$$

and

$$\mathbf{B(x)} = -\sum_{\mathbf{i}} (\mathbf{e})_{\mathbf{i}} \cdot \nabla \times \mathbf{N_i(x)}. \quad (4)$$

Particle-In-Cell (PIC) Method

Numerical charge conservation is of utmost importance in all PIC methods where current $\mathbf{J}$ and charge ρ densities are deposited on the computational grid. First, the field propagation must not accumulate spurious charges. Second, the discrete analog of the continuity equation

$$\frac{\partial \rho}{\partial t} + \nabla \cdot \mathbf{J} = \mathbf{0}$$

D05 Code Developments and Simulation Techniques

must hold. Third, initial conditions need to fulfill the discrete analogs of the two Maxwell divergence equations $\nabla \cdot \mathbf{B} = \mathbf{0}$ and $\nabla \cdot \mathbf{E} = \rho$. In our approach, these conditions are satisfied by using Whitney basis functions and starting with a charge-free simulation domain.

The particle distribution is modeled by a number of macro particles specified by position $\mathbf{x}$, momentum $\mathbf{p}$, rest mass m and charge q attributes. The total current density is then approximated as

$$\mathbf{J}(\mathbf{x}, t) = \sum_i \rho(\mathbf{x} - \mathbf{x_i}, t) \cdot \mathbf{v_i}(t),$$

with $\mathbf{v} = \frac{\mathbf{p}}{\gamma m}$, $\gamma^2 = 1 + |\frac{\mathbf{p}}{mc}|^2$ and ρ the macro particle charge density, currently implemented for point charges and Gaussian line currents (act as smoothing filter).

The macro particles obey the classical relativistic collision-less (Newton-Lorentz) equations of motion,

$$\frac{d\mathbf{r}}{dt} = \mathbf{v},$$
$$\frac{d\mathbf{p}}{dt} = q(\mathbf{E} + \mathbf{v} \times \mathbf{B}),$$

which are integrated using the standard 'Boris' pusher, an explicit method splitting the momentum update into two electric accelerations and an intermediate magnetic rotation [3]. For simplicity, the same time step is used for the field solver and for the particle pusher. This is reasonable when space charge effects are significant, especially since the electromagnetic fields are readily available without the need for interpolations, cf. Eqs. (3) and (4).

hpq-refinement

It is well known that FE methods are most efficient when using (adaptive) hpq-refinement, where h stands for the grid resolution, p for the polynomial order of the basis functions and q for the degree of mesh curvature. Our current implementation supports static h- and q-refinement (q=1,2) as well as adaptive p-refinement (p=1...6), where each element is assigned an independent value of p and its basis functions that are shared with neighboring elements are restricted to the highest common order. This requires a consistent set of hierarchical FE basis functions.

Higher-order elements not only significantly improve field accuracy and dispersive properties [4], but they also generically lead to higher-order accurate, self-consistent particle-field coupling equivalent to, but much less laborious than, complicated higher-order interpolation schemes commonly found in finite-difference methods [5].

For illustration, when modeling a rotationally symmetric problem in 2D, the electric field and current density in a typical p^{th}-order Whitney element are determined by weighted sums over $\frac{3}{2}p^2 + \frac{7}{2}p + 1$ different basis functions (e.g. 76 for 6th-order), cf. Eq. (3).

Note that potentially orders of magnitude in computational resources can be saved, while preserving full simulation accuracy, by restricting higher-order p-refinement

to regions that are inside the causal range of the particle bunch. Since a change of the selected basis functions requires reassembly of the system matrix, adaptive p-refinement is usually only done from time to time, in coordination with the particle dynamics. Fig. 1 shows an example mesh with adaptive p-refinement.
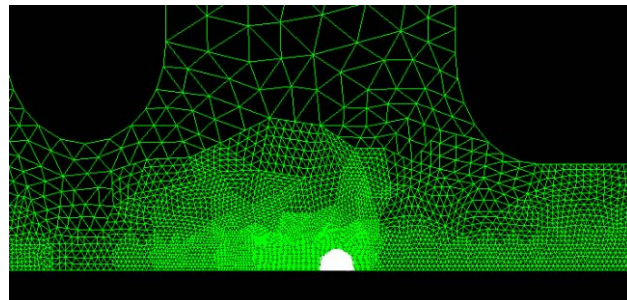
Figure 1: Adaptive p-refinement in an unstructured 2D mesh model of LCLS RF gun. For visualization, each element of order p is divided into p^2 sub-triangles and curved boundaries are drawn as straight lines.

RESULTS

In the following, PIC simulations of the 1.6 cell S-band LCLS RF gun are presented [6].

LCLS RF Gun PIC Simulations

In the simulations, the gun is driven by the π-mode with a peak accelerating field gradient of 120 MV/m at the cathode. A cold, uniform, 10 ps long (flat-top), cylindrically symmetric electron bunch of 1 mm radius is emitted from a flat cathode, centered around a phase of -58° with respect to the crest. Bunch charges are varied from zero space charge (10^{-6} nC) up to 1.5 nC. Although Pic2P fully supports external magnetostatic fields, the small solenoidal fringe field inside the gun region is not included here for simplicity. A conformal, unstructured rotationally symmetric (2D) mesh model of the LCLS RF gun is used, similar to Fig. 1, and cavity modes are obtained with the integrated parallel FE frequency domain code Omega2P. Fig. 2 shows the particle
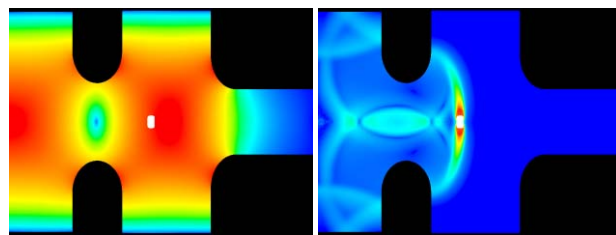
Figure 2: Cross-section of LCLS RF gun, showing electric field magnitude as calculated with Pic2P. (Left) Particle bunch accelerated by operating mode, (Right) scattered fields from interactions of bunch with gun cavity.

bunch accelerated by the driven cavity mode and the scattered fields generated by the beam in its interaction with the gun cavity. Fig. 3 shows the evolution of the normal-

Normalized Transverse RMS Emittance vs Z
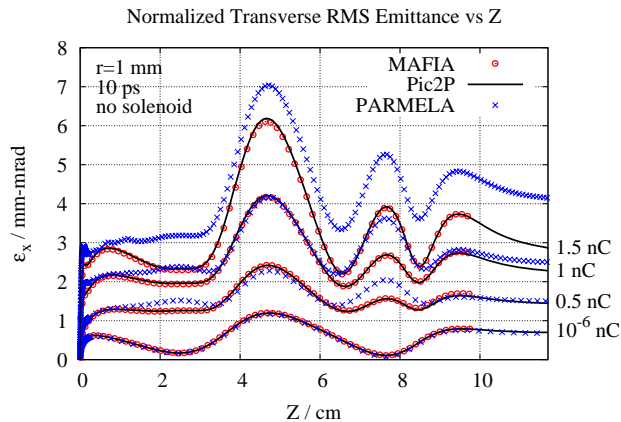
Figure 3: Comparison of normalized transverse RMS emittance vs mean longitudinal position in LCLS RF gun as calculated by MAFIA, Pic2P and PARMELA for different bunch charges.

ized transverse RMS emittance during transit through the gun for different bunch charges. There is excellent agreement between Pic2P and MAFIA, but PARMELA differs as soon as space charge effects are significant, presumably because it ignores wakefield and retardation effects, as detailed in a previous study[7].

Pic2P converges very quickly, requiring less CPU time and two orders of magnitude fewer DOFs than MAFIA, cf. Fig. 4. While particle-related computations usually

Normalized Transverse RMS Emittance vs Z
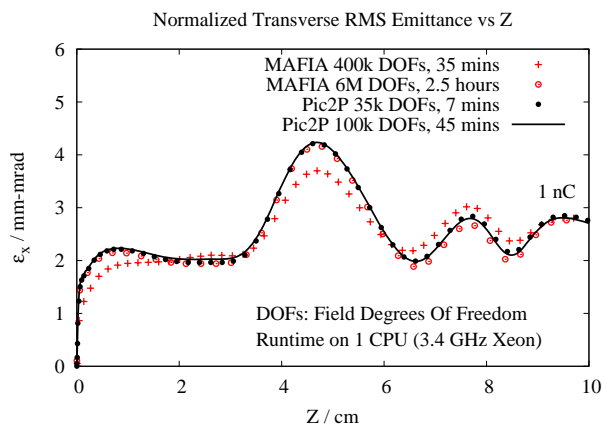
Figure 4: Convergence of normalized transverse RMS emittance in LCLS RF gun with MAFIA and Pic2P for different problem sizes and runtimes.

dominate the runtime on a single CPU, they can be efficiently parallelized by distributing the particles and communicating the fields, and parallel speedup becomes dominated by the scalability of the linear solver. Using parallel processing, highly accurate results can be obtained with Pic2P in a few minutes.

05 Beam Dynamics and Electromagnetic Fields

CONCLUSIONS

The parallel finite element electromagnetic PIC code Pic2P, the first such successful implementation, was used to model space charge effects in the LCLS RF gun from 1st principles. Pic2P shows excellent agreement to MAFIA, while offering much faster convergence. A powerful combination of conformal grids, unconditionally stable time-integration, higher-order basis functions with adaptive p-refinement leads to a highly efficient use of computational resources. Parallel processing further reduces runtimes down to only a few minutes for a fully converged result. Petascale computing will allow accurate start-to-end simulations of photoinjectors.

Results from the electrostatic code PARMELA differ whenever wakefield and retardation effects are important. This indicates the significance of self-consistent simulations for the design of high-brightness, low-emittance electron guns, for use in next-generation free-electron lasers and light sources.

ACKNOWLEDGMENTS

REFERENCES

[1] K. Ko et al., "SciDAC and the International Linear Collider: Petascale Computing for Terascale Accelerator", Invited Talk given at SciDAC 2006 Conference, Denver, Colorado, June 25-29, 2006.

[2] N. M. Newmark, "A method of computation for structural dynamics", Journal of Eng. Mech. Div., ASCE, vol. 85, pp. 67-94, July 1959.

[3] J. P. Boris, "Relativistic plasma simulation-optimization of a hybrid code", Proc. Fourth Conf. Num. Sim. Plasmas, Naval Res. Lab, Wash. D.C.,pp. 3-67, Nov. 2-3, 1970.

[4] M. Ainsworth, "Dispersive properties of high-order Nedelec/edge element approximation of the time-harmonic Maxwell equations", Philos. trans.-Royal Soc., Math. phys. eng. sci., vol. 362, no. 1816, pp. 471-492, 2004.

[5] O. Buneman, W. Pardo, "Fast numerical procedures for computer experiments on relativistic plasmas", Relativistic Plasmas(The Coral Gables Conference, University of Miami), W. A. Benjamin, New York, pp. 205-219, 1968.

[6] L. Xiao et al., "Dual Feed RF Gun Design for the LCLS", Proc. PAC 2005, Knoxville, Tennessee, May 15-20, 2005.

[7] A. Candel et al., "Parallel Higher-order Finite Element Method for Accurate Field Computations in Wakefield and PIC Simulations", Proc. ICAP 2006, Chamonix Mont-Blanc, France, October 2-6, 2006.

D05 Code Developments and Simulation Techniques